Appl. Phys. B 67, 733–741 (1998)

Applied Physics B
Lasers
and Optics

Quantum trajectories of interacting pseudo-spin networks

C.M. Granzow, G. Mahler*

Institut für Theoretische Physik, Universität Stuttgart, Pfaffenwaldring 57, 70550 Stuttgart, Germany
(Fax: +49-711/685-4909, E-mail: claus@theo.physik.uni-stuttgart.de)

Received: 12 June 1998

Abstract. We consider quantum trajectories of composite systems as generated by the stochastic unraveling of the respective Lindblad master equation. Their classical limit is taken to correspond to local jumps between orthogonal states. Based on statistical distributions of jump- and inter-jump distances we are able to quantify the non-classicality of quantum trajectories. To account for the operational effect of entanglement we introduce the novel concept of "co-jumps".

PACS: 42.50.Lc; 06.20.Dk

In contrast to the ensemble description based on master equations, quantum trajectories make available further information about details that are lost by ensemble averaging. The study of quantum trajectories of open systems [1, 2] has therefore found broad application in various fields to analyze fundamental processes.

It is important to distinguish the quantum trajectories in Hilbert space from the Feynman paths [3]. Whereas the latter are defined in the underlying classical phase space and contribute with a complex probability amplitude to the path integral, the Hilbert space quantum trajectories contribute with a real and positive probability to the ensemble density matrix [4].

Hence in the Feynman path integral formulation the classical limit can be obtained in a direct way when the interferences between the paths basically reduce to the classical path. In contrast the Hilbert space does not have a direct classical analogue. Here, we define a Hilbert space trajectory as "classical" if it is constrained to orthogonal states. The jumps in the Hilbert space imply jumps in observable space such as energy or angular momentum. The orthogonal states can then be interpreted as the eigenstates of some observable, its spectrum will here be taken to be discrete and finite ("telegraph signal").

* Corresponding author

While the non-classicality of states has attracted much interest recently [5–9], the non-classicality of the dynamical evolution, in particular on the level of trajectories, has received little if any attention so far. It is tempting to expect that an increasing dissipative interaction with the classical environment should make the trajectories more and more "classical". One may wonder, however, to what extent this expectation can be verified quantitatively. One may also wonder whether there is a relationship between non-classicality of states and of trajectories.

In this paper we introduce statistical distribution functions to account for the non-classicality of quantum trajectories, and show their properties and their relation to the non-classicality of states.

This paper is organized as follows. In Sect. 1 we define a convenient operator set for the description of quantum networks, the states of which will be discussed in Sect. 2. The unraveling of the Linblad master equation into single quantum trajectories is summarized in Sect. 3.1. In Sect. 3.2 we discuss some properties of the measure of state distance, which are applied to the quantum trajectories in Sect. 3.3 and Sect. 3.4. The concept of jump- and co-jump distances is exemplified in Sect. 4 for special two-, three-, and four-particle states. In Sect. 5 we present numerical results exploiting this jump concept for simulated trajectories. We conclude with a brief summary.

1 Cluster operators

We consider a network consisting of N subsystems of n states each. The local states are $|p(\mu)\rangle$, $p = 1, 2, \ldots, n$, $\mu = 1, 2, \ldots, N$, allowing us to introduce the transition operators $\hat{P}_{pq}(\mu) = |p(\mu)\rangle\langle q(\mu)|$. These can be combined to give the n^2 generators of the SU(n) algebra, which read for $n = 2$:

$$\hat{\lambda}_1(\mu) = \hat{P}_{12}(\mu) + \hat{P}_{21}(\mu), \tag{1}$$

$$\hat{\lambda}_2(\mu) = i\left(\hat{P}_{12}(\mu) - \hat{P}_{21}(\mu)\right), \tag{2}$$

$$\hat{\lambda}_3(\mu) = \hat{P}_{22}(\mu) - \hat{P}_{11}(\mu), \tag{3}$$

$$\hat{\lambda}_0(\mu) = \hat{P}_{11}(\mu) + \hat{P}_{22}(\mu) = \hat{1}(\mu). \tag{4}$$

They constitute a complete, orthogonal set of $n^2 - 1$ traceless operators. A corresponding set for the total network is then given by the n^{2N} product operators. Here we will restrict ourselves to $N = 4$, $n = 2$, in which case we have [10]

$$\hat{Q}_{mlkj} = \hat{\lambda}_m(4) \otimes \hat{\lambda}_l(3) \otimes \hat{\lambda}_k(2) \otimes \hat{\lambda}_j(1). \tag{5}$$

The number c of indices not equal to zero is the number of subsystems this operator acts on. There are $n_c = \binom{N}{c}(n^2-1)^c$ such c cluster operators, with $0 \le c \le N$. Operators $\hat{Q}$ acting on different subsystems commute.

2 Quantum states

2.1 Correlations

Any network operator in a given Liouville space $\{N, n\}$ can be expressed in terms of such cluster operators. In particular, for the density operator $\hat{\rho}$ one finds (again for $N = 4$, $n = 2$, cf. [10])

$$\hat{\rho} = \frac{1}{2^4} \sum_{jklm} K_{mlkj} \hat{Q}_{mlkj}, \tag{6}$$

with $K_{mlkj} = \mathrm{tr}\left\{\hat{\rho}\hat{Q}_{mlkj}\right\}$.

These expectation values $\boldsymbol{K} = \left\{K_{mlkj}\right\}$ uniquely specify the state; they decompose into n_c c-point correlation functions. The only $c = 0$ term is $K_{0000} = \mathrm{tr}\{\hat{\rho}\} = 1$. The $c = 1$ terms are the (local) Bloch vectors, $K_{000j} \equiv \lambda_j^{(1)}$, $K_{00k0} \equiv \lambda_k^{(2)}$ etc., which can be found from local (ensemble)measurements. The $c > 1$ terms are typically inferred from coincidence measurements (ensemble measurements).

2.2 Covariances

One easily convinces oneself that these correlation functions K_{mlkj} factorize if and only if the state $\hat{\rho}$ exhibits some product form. For example, if $\hat{\rho}(4,3,2,1) = \hat{\rho}(4,2) \otimes \hat{\rho}(3,1)$, then

$$K_{mlkj} = K_{m0k0} \times K_{0l0j} \tag{7}$$

or if $\hat{\rho}(4,3,2,1) = \hat{\rho}(4) \otimes \hat{\rho}(3,2) \otimes \hat{\rho}(1)$, then

$$K_{mlkj} = K_{m000} \times K_{0lk0} \times K_{000j} \quad \text{etc.} \tag{8}$$

Subsystems and groups of subsystems which do *not* factor are called "entangled" ($\hat{\rho}$ of the total system is taken to be pure and to describe a single network). Without any entanglement, all c-point correlation functions are thus reducible to local expectation values (i.e. of type $c = 1$).

It is therefore convenient to introduce state parameters, which describe deviations from this factorization property. For this purpose we introduce a supplementary set of cluster operators

$$\Delta\hat{Q}_{mlkj} = \Delta\hat{\lambda}_m(4) \otimes \Delta\hat{\lambda}_l(3) \otimes \Delta\hat{\lambda}_k(2) \otimes \Delta\hat{\lambda}_j(1), \tag{9}$$

based on the local "deviation-operators"

$$\Delta\hat{\lambda}_m(\mu) = \begin{cases} \hat{\lambda}_m(\mu) - \lambda_m^{(\mu)}\hat{1}(\mu) & \text{for } m \neq 0 \\ \hat{1}(\mu) & \text{for } m = 0 \end{cases}. \tag{10}$$

The respective expectation values ("quantum covariances")

$$M_{mlkj} = \mathrm{tr}\left\{\Delta\hat{Q}_{mlkj}\hat{\rho}\right\} \tag{11}$$

then also come in different c classes: For $c = 0$, $M_{0000} = K_{0000} = 1$, for $c = 1$, $M_{000j} = 0$ etc., for $c = 2$,

$$M_{00kj} = K_{00kj} - K_{00k0} \times K_{000j} \quad \text{etc.} \tag{12}$$

for $c = 3$,

$$\begin{aligned} M_{0lkj} =& K_{0lkj} - K_{0lk0} \times \lambda_j^{(1)} - K_{0l0j} \times \lambda_k^{(2)} \\ & - K_{00kj} \times \lambda_l^{(3)} + 2\lambda_l^{(3)} \times \lambda_k^{(2)} \times \lambda_j^{(1)} \quad \text{etc.} \end{aligned} \tag{13}$$

The set of expectation values $\{\lambda_k^{(\mu)}, M_{mlkj}\}$ can alternatively be used to specify the network state. With all $\lambda_k^{(\mu)} = 0$ we obviously have $M_{mlkj} = K_{mlkj}$. The factoring properties of K_{mlkj} carry over to M_{mlkj}. In particular, under the condition as for (8) we get $M_{mlkj} = M_{m000} \times M_{0lk0} \times M_{000j} = 0$. In general, any specific M_{mlkj} is zero, if at least one individual subsystem entering with a local operator-index $\neq 0$ factors out.

2.3 Entanglement measures

For a product state as of (7) we have $M_{mlkj} = M_{m0k0} \times M_{0l0j} \neq 0$. By substracting all possible partitions ($c = c_1 + c_2 + \ldots$, $c_i \ge 2$) we introduce (here for $c = 4 = 2 + 2$):

$$\begin{aligned} \tilde{M}_{mlkj} = M_{mlkj} & - M_{ml00}M_{00kj} \\ & - M_{m0k0}M_{0l0j} \\ & - M_{m00j}M_{0lk0}, \end{aligned} \tag{14}$$

which is thus zero for *any* product state. For $c < 4$ we obviously get $\tilde{M} = M$; for $c > 4$ this connection scheme is easily generalized.

To quantify entanglement on the total network-level ($N = 4$) we use (cf. [10])

$$\beta(4,3,2,1) = \sum_{m,l,k,j=1}^{3} \left(\tilde{M}_{mlkj}\right)^2, \tag{15}$$

as well as corresponding sub-space measures such as

$$\beta(2,1) = \sum_{k,j=1}^{3} \left(\tilde{M}_{00kj}\right)^2. \tag{16}$$

Note that $\beta(2,1) \neq 0$ indicates any entanglement $\tilde{M}_{00kj} \neq 0$ between subsystems (2) and (1) only: $\beta(4,3,2,1)$ could still be zero. These β functions can be used instead of the "entropies of entanglement" (= entropy of the respective reduced density operators) [5, 6]; the M terms are easier to calculate and, furthermore, can be made the basis of approximation schemes (see below).

3 Quantum trajectories

3.1 Stochastic unraveling

The evolution of open quantum systems is usually approximated by the Lindblad master equation, which is Markovian. Here, the influence of the environment is specified by so-called environment operators $\hat{L}_s$ and the corresponding damping rates W_s:

$$\frac{\partial}{\partial t}\hat{\rho}+\frac{i}{\hbar}\left[\hat{H},\hat{\rho}\right]=\sum_s\left(-\frac{1}{2}W_s\left\{\hat{L}_s^+\hat{L}_s\hat{\rho}+\hat{\rho}\hat{L}_s^+\hat{L}_s\right\}+W_s\hat{L}_s\hat{\rho}\hat{L}_s^+\right). \tag{17}$$

Those operators $\hat{L}_s$ play a crucial role in the stochastic unraveling of the master equation. The coupling to the environment leads to individual quantum jumps between which there is a non-unitary continuous evolution [1]. The jumps are generated by the last term of the right-hand side whereas the first two terms can be combined with the Hamilton operator into a non-Hermitian effective Hamiltonian responsible for the continuous inter-jump evolution. The probability for a quantum jump of type s after the time interval δt is given by

$$p_s=W_s\mathrm{tr}\left\{\hat{L}_s\hat{\rho}\hat{L}_s^+\right\}\delta t\,. \tag{18}$$

We assume that these projections can be expressed in terms of, in general, non-Hermitian operators, $\hat{L}_s=\hat{P}_s(\mu)$, which are taken to act locally on one of the subsystems (μ),

$$\hat{\rho}'=\frac{\hat{P}_s(\mu)\hat{\rho}\hat{P}_s(\mu)^+}{\mathrm{tr}\left\{\hat{P}_s(\mu)\hat{\rho}\hat{P}_s(\mu)^+\right\}}. \tag{19}$$

For the characterization of these pure-state trajectories the timing of jumps plays a central role because it may give rise to measurable events and to count- and waiting-time statistics [11]. Unfortunately, however, these give only indirect evidence for the non-classicality of trajectories (for example, anti-bunching). We therefore propose to supplement the analysis by directly referring to the motion in Liouville space.

The characterization of single quantum trajectories with respect to classicality measures could be done in different ways. In addition to the possibilities presented below one may think of calculating the distribution functions of local as well as non-local coherence measures (cf. Sect. 2.3). However, it should be noted that these properties depend on the basic operators chosen for the state description. In the case that the coupling to the environment leads to the build-up of states that do not happen to coincide with eigenstates of the local operators $\hat{\lambda}_3(\mu)$, this approach will not show a classical limit (i.e. α and/or β remain not equal to zero).

3.2 Measures of state distance

There have been different proposals for defining a metric for density matrices (see, for example, the Bures metric [12], fidelity [13] or mutual information [5]). For the non-orthogonal Glauber states $|\alpha\rangle$, for example, a "distance" d has been proposed [14] with $|\langle\alpha|\alpha'\rangle|^2=\exp\{-d^2\}$. In this paper we use a measure, D, for the distance between two arbitrary (generally mixed) states $\hat{\rho}$ and $\hat{\rho}'$ according to

$$D^2_{\hat{\rho}\hat{\rho}'}=\mathrm{tr}\{(\hat{\rho}-\hat{\rho}')^2\}, \tag{20}$$

which is, independent of the dimension of the Liouville space, between 0 and 2. The maximum (squared) distance of 2 applies to orthogonal states. In the case of pure states ($\hat{\rho}=|\Psi\rangle\langle\Psi|$), $D^2_{\hat{\rho}\hat{\rho}'}$ can be rewritten as :

$$D^2_{\Psi\Psi'}=2(1-|\langle\Psi|\Psi'\rangle|^2)\,. \tag{21}$$

It is easy to show that $D_{\hat{\rho}\hat{\rho}'}$ satisfies the metric properties [15] in the Liouville space $\mathcal{L}$, i.e.

$$\begin{aligned}
&D_{\hat{\rho}\hat{\rho}'}\geq 0 \quad \text{for all } \hat{\rho},\,\hat{\rho}' \text{ of } \mathcal{L},\\
&D_{\hat{\rho}\hat{\rho}'}=0 \quad \text{if and only if } \hat{\rho}=\hat{\rho}',\\
&D_{\hat{\rho}\hat{\rho}'}=D_{\hat{\rho}'\hat{\rho}} \quad \text{for all } \hat{\rho},\,\hat{\rho}' \text{ of } \mathcal{L},\\
&D_{\hat{\rho}\hat{\rho}'}\leq D_{\hat{\rho}\hat{\rho}''}+D_{\hat{\rho}''\hat{\rho}'} \quad \text{(triangle inequality)}.
\end{aligned} \tag{22}$$

This measure $D^2_{\hat{\rho}\hat{\rho}'}$ can directly be expressed in terms of the SU(2) parameters, K_{mlkj}, namely as the squared length of the difference vector between $\boldsymbol{K}=\{K_{mlkj}\}$ and $\boldsymbol{K}'=\{K'_{mlkj}\}$,

$$D^2_{\hat{\rho}\hat{\rho}'}=\frac{1}{2^4}\sum_{j,k,l,m=0}^{3}\left(K_{mlkj}-K'_{mlkj}\right)^2. \tag{23}$$

This concept of state distance can easily be generalized to distances defined on reduced state spaces: Observing that, for example,

$$\mathrm{tr}_{\{4,3,2\}}\left\{\hat{Q}_{mlkj}\right\}=\hat{\lambda}_j(1)2^3\delta_{m0}\delta_{l0}\delta_{k0}, \tag{24}$$

(here $\mathrm{tr}_{\{\mu\}}$ means trace operation within μ-subspace only), we find for the reduced density operator of subsystem (1), say,

$$\hat{\rho}(1)=\mathrm{tr}_{\{432\}}\hat{\rho}=\frac{1}{2}\sum_j K_{000j}\hat{\lambda}_j(1) \tag{25}$$

and

$$\left(D^{(1)}_{\{\hat{\rho},\hat{\rho}'\}}\right)^2=\frac{1}{2}\sum_j\left(K_{000j}-K'_{000j}\right)^2. \tag{26}$$

Correspondingly, the distance as seen from the subsystems (4, 3, 2) is

$$\left(D^{(4,3,2)}_{\{\hat{\rho},\hat{\rho}'\}}\right)^2=\frac{1}{2^3}\sum_{k,l,m}\left(K_{mlk0}-K'_{mlk0}\right)^2. \tag{27}$$

Then we have by inspection the inequality

$$\frac{1}{2^3}\left(D^{(1)}_{\{\hat{\rho},\hat{\rho}'\}}\right)^2+\frac{1}{2}\left(D^{(4,3,2)}_{\{\hat{\rho},\hat{\rho}'\}}\right)^2\leq D^2_{\{\hat{\rho},\hat{\rho}'\}}. \tag{28}$$

3.3 State-distance distributions

In order to characterize quantum trajectories we introduce various types of state distances: the "jump distance", by inserting into (21) the state right before and after the jump (in analogy to the jump distance of the Brownian motion in classical physics [16]), the "inter-jump distance" as the distance between the final state of the last jump and the initial state of the following jump, and the state distance for a specified time interval τ during the evolution of a given quantum trajectory,

$$D_\tau^2 = \mathrm{tr}\left\{\left(\hat{\rho}(t) - \hat{\rho}(t+\tau)\right)^2\right\}. \tag{29}$$

Finally, we will be interested not only in the jump distance of the total system, but also of parts of the system in their respective reduced space μ. Therefore we use $\left(D^{(\mu)}_{\{\hat{\rho}\hat{\rho}'\}}\right)^2$ as defined in (26) and (27) where $\hat{\rho}$ ($\hat{\rho}'$) is the total density operator before (after) jump. In this way we can test to what extent a projection in subspace (ν; $\nu \neq \mu$) affects the reduced state of subsystem μ ("co-jumps").

Sampling over one individual trajectory we find the corresponding distribution functions, $f(D^2)$. These are normalized:

$$\int_0^2 f(D^2)\,\mathrm{d}(D)^2 = 1. \tag{30}$$

3.4 Co-jumps and entanglement

One easily shows that for any complete (POVM)-type measurement [17], the *ensemble-averaged* co-jump must be zero. For this purpose we write, for the (ensemble) density operator after measurement in (2,1), for example

$$\hat{\rho}' = \sum_s \hat{P}_s(2,1)\hat{\rho}\hat{P}_s^+(2,1), \tag{31}$$

with $\sum_s \hat{P}_s^+(2,1)\hat{P}_s(2,1) = \hat{1}$ and consider (overlines indicate ensemble-averaging)

$$\begin{aligned}
\overline{K}'_{ml00} &= \mathrm{tr}\left\{\hat{\rho}'\hat{Q}_{ml00}\right\} && (32)\\
&= \mathrm{tr}\left\{\sum_s \left(\hat{P}_s(2,1)\hat{\rho}\hat{P}_s^+(2,1)\hat{Q}_{ml00}\right)\right\} && (33)\\
&= \mathrm{tr}\left\{\sum_s \left(\hat{P}_s^+(2,1)\hat{P}_s(2,1)\right)\hat{\rho}\hat{Q}_{ml00}\right\} && (34)\\
&= \mathrm{tr}\left\{\hat{\rho}\hat{Q}_{ml00}\right\} = \overline{K}_{ml00}. && (35)
\end{aligned}$$

Here we have made use of the fact that $\hat{P}_s^+(2,1)$ and $\hat{Q}_{ml00}$ commute as they act on different sub-spaces. We conclude that

$$\left(D^{(4,3)}_{\{\hat{\rho}\hat{\rho}'\}}\right)^2 = \frac{1}{2^2}\sum_{ml}\left(\overline{K}_{ml00} - \overline{K}'_{ml00}\right)^2 = 0. \tag{36}$$

This means that ensemble quantum mechanics is local in an operational sense: Measuring in some sub-space, here (2,1), does not have any influence outside this subspace. An analogue statement holds for respective unitary transformations.

However, as is known since the famous EPR experiments [18] individual measurements leading to new information may violate this locality. To show this we consider

$$\hat{\rho}' = \frac{1}{p_s}\hat{P}_s(2,1)\hat{\rho}\hat{P}_s^+(2,1), \tag{37}$$

where $p_s = \mathrm{tr}\left\{\hat{P}_s^+(2,1)\hat{P}_s(2,1)\hat{\rho}\right\}$. Based on the same arguments as before we obtain

$$\begin{aligned}
K'_{ml00} = K_{ml00} + \frac{1}{p_s}\mathrm{tr}\Big\{\hat{\rho}\left(\hat{Q}_{ml00} - \hat{1}K_{ml00}\right)\\
\times \hat{P}_s^+(2,1)\hat{P}_s(2,1)\Big\}.
\end{aligned} \tag{38}$$

Now let $\hat{P}_s^+\hat{P}_s = \frac{1}{2}\left(\hat{1}(1) + \hat{\lambda}_3(1)\right) = \hat{P}_{22}(1)$. Then we get

$$K'_{ml00} - K_{ml00} = \frac{1}{2p_s}\left(K_{ml03} - K_{ml00}\times K_{0003}\right). \tag{39}$$

The right-hand side is zero if $K_{ml03} = K_{ml00}\times K_{0003}$, i.e. if subsystem (1), which is measured, has no entanglement with the subsystem (4,3). Otherwise,

$$\left(D^{(4,3)}_{\{\hat{\rho}\hat{\rho}'\}}\right)^2 = \frac{1}{2^2}\sum_{ml}\left(K_{ml00} - K'_{ml00}\right)^2 \neq 0, \tag{40}$$

which is thus non-zero also for the ensemble. Comparing with (36) we note that

$$\overline{\left(K_{ml00} - K'_{ml00}\right)^2} \neq \left(\bar{K}_{ml00} - \bar{K}'_{ml00}\right)^2. \tag{41}$$

4 Co-jump properties of model states

Our intention is to use the concept of co-jumps for the characterization of single quantum trajectories. As these trajectories always connect pure states, "mixed states" only appear for reduced sub-spaces. Any non-zero entropy of such reduced density matrices is due to entanglement and not due to our incomplete knowledge. Co-jumps will occur also within reduced spaces; such situations will be included below in a formal way.

In the following we perform individual "measurements" based on the specific operators (cf. (19))

$$\hat{P}_i(\mu) = \frac{1}{2}\left(\hat{1}(\mu) + \hat{\lambda}_i(\mu)\right), i = 0,1,2,3\,. \tag{42}$$

Note that these measurements correspond to only one outcome each. In the case of coincidence measurements we take the dyadic product of such single particle operators. According to (23), (26) and (27) we then calculate the jump- and co-jump distance.

Table 1. (Squared) jump distances for the specific $N = 2$ particle state $\hat{\rho}_x$ (see (43)) (projection by $\hat{P}_i^{(2)}$)

x	i	$\left(D^{(1)}\right)^2$	$(D)^2$
1	1	0.5	1.0
1	2	0.5	1.0
1	3	0.5	1.0
0	1	0.0	0.25
0	2	0.0	0.25
0	3	0.0	0.25

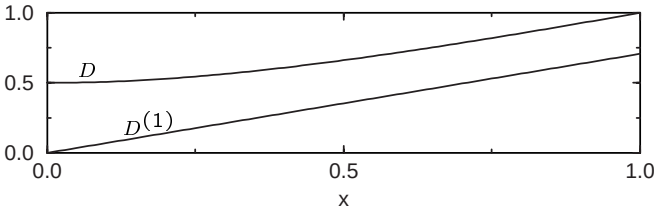

Fig. 1. Co-jump $D^{(1)}$ and total jump D for the Werner state $\hat{\rho}_x$ which is projected by $\hat{P}_i^{(2)}$ ($x = 1 \rightarrow$ EPR state)

4.1 Two-particle state

We first consider the completely mixed state, the EPR state ("cat state") $|\mathrm{EPR}\rangle = \frac{1}{\sqrt{2}}(|12\rangle - |21\rangle)$, and the "Werner state" [8]

$$\hat{\rho}_x = (1-x)\frac{1}{4}\hat{1} + x|\mathrm{EPR}\rangle\langle\mathrm{EPR}|\,, \quad 0 \le x \le 1\,. \tag{43}$$

The maximum entanglement for the latter is reached for $x = 1$ (EPR state, $\beta(2, 1) = 3$). Table 1 shows results for $x = 0$ and $x = 1$, conditioned by the respective projection, i. Jump and co-jump are independent of i, confirming the "isotropy" of the EPR state and of the mixed state.

In Fig. 1 one can see the transition from the mixed state to the EPR state. In contrast to D, the co-jump $D^{(1)}$ is linear in the whole region from $x = 0$ to $x = 1$. The state (43) reacts in a local way for $x = 0$ only.

The non-locality, to be sure, could still be "explained" by a local hidden-variable theory [6] unless $x > 1/\sqrt{2}$ (violation of Bell inequalities) or $x > 1/3$ (violation of separability condition [7]), respectively. These interpretations have to assume, though, that mixed states can be treated as classical mixtures (i.e. resulting from our ignorance [19] rather than from undefined properties due to entanglement with other subsystems). Stochastic modeling deals with single networks and individual subsystems (additional knowledge!); co-jumps within the latter then reflect their ("objective") change as induced by a distant observation.

4.2 Three-particle state

As a representative for the N=3 case we consider the cat state (GHZ state, $\beta(3, 2, 1) = 4$, $\beta(2, 1) = 1$),

$$|\mathrm{GHZ}\rangle = \frac{1}{\sqrt{2}}(|111\rangle + |222\rangle)\,, \tag{44}$$

Table 2. (Squared) jump distances for the $N = 3$ cat state (projection by $\hat{P}_i^{(2)} \otimes \hat{P}_j^{(3)}$)

i	j	$\left(D^{(1)}\right)^2$	$\left(D^{(1,2)}\right)^2$	$(D)^2$
0	1	0.0	0.5	1.0
0	2	0.0	0.5	1.0
0	3	0.5	0.5	1.0
1	1	0.5	–	1.5
1	2	0.5	–	1.5
1	3	0.5	–	1.5
3	1	0.5	–	1.5
3	2	0.5	–	1.5
3	3	0.5	–	1.0

Table 3. (Squared) jump distances for the $N = 4$ cat state (projection by $\hat{P}_i^{(3)} \otimes \hat{P}_j^{(4)}$)

i	j	$\left(D^{(1)}\right)^2$	$\left(D^{(1,2)}\right)^2$	$(D)^2$
0	1	0.0	0.0	1.0
0	2	0.0	0.0	1.0
0	3	0.5	0.5	1.0
1	1	0.0	0.5	1.5
1	2	0.0	0.5	1.5
1	3	0.5	0.5	1.5
3	1	0.5	0.5	1.5
3	2	0.5	0.5	1.5
3	3	0.5	0.5	1.0

and study projections on particle 3, and on particles 2 and 3 in coincidence. In contrast to the EPR state, the GHZ state is not rotationally invariant, the $i = 3$ direction plays a special role which can be seen by comparing the result for $(i, j) = (0, 1)$ and $(0, 3)$ or $(1, 1)$, $(3, 3)$ (see Table 2).

One should note that the reduced state $\hat{\rho}(3, 1)$ could be written as a mixed product state (i.e. separable in the sense of [7]), which, nevertheless, leads to a co-jump in (1) induced by subsystem (3). Only without further knowledge could this effect be interpreted as being due to classical correlations, cf. Sect. 4.1.

4.3 Four-particle state

The special four-particle "cat state" ($\beta(4, 3, 2, 1) = 12$, $\beta(3, 2, 1) = 0$, $\beta(2, 1) = 1$),

$$|\Psi_{\mathrm{Cat}}\rangle = \frac{1}{\sqrt{2}}(|1111\rangle + |2222\rangle)\,, \tag{45}$$

shows a co-jump behavior which is, contrary to the $N = 3$ cat state, different also for $(i, j) = (1, 1)$ and $(1, 3)$. The pertinent co-jump properties of this state are summarized in Table 3.

5 Jump statistics of simulated trajectories

5.1 Hamilton model

In our simulations we consider an open quantum network consisting of pseudo spins (two-level systems) which interact with each other, with external electro-magnetic fields and

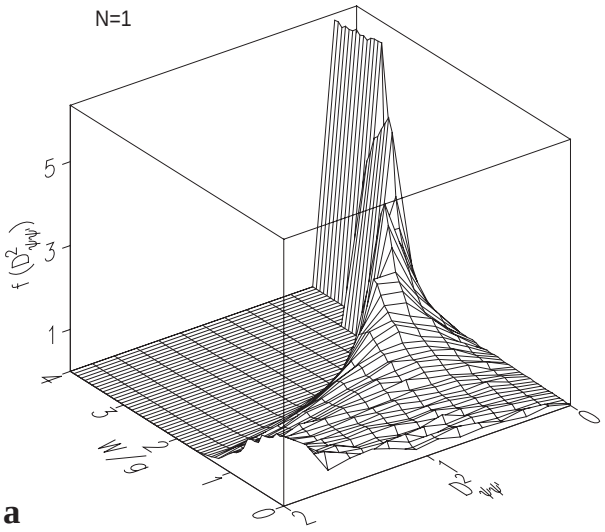

a

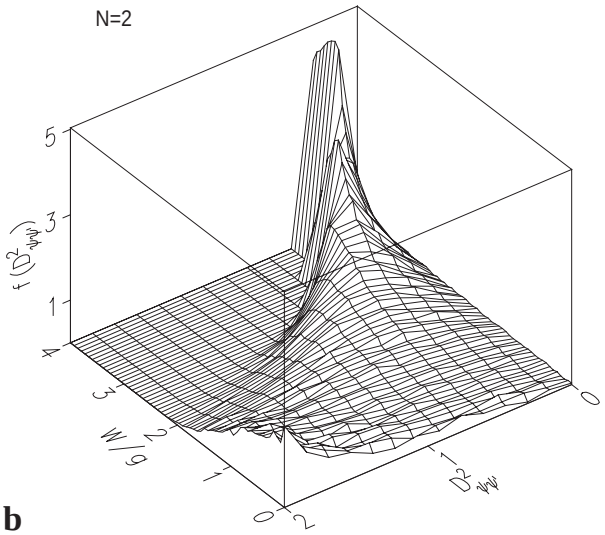

b

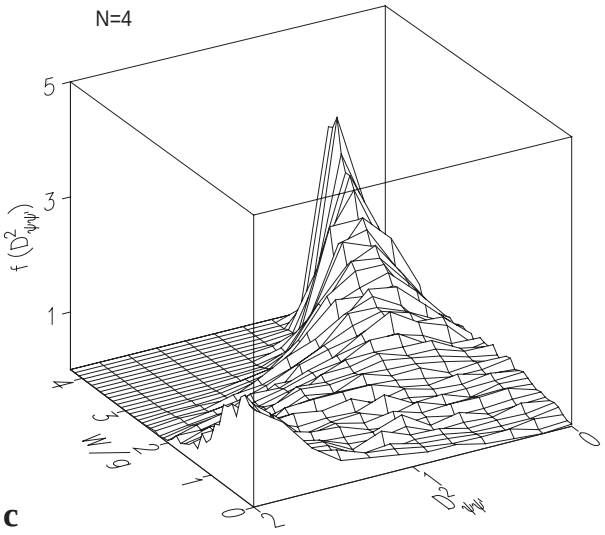

c

Fig. 2. Distribution function $f(D^2_{\psi\psi'})$ for the jump distance D of a homogeneous network N in interaction with a bath at $T = 0$ (damping rate $W^{\mu}_{\downarrow} = W$, $g^{\mu} = g =$ coupling parameter to the coherent driving field, coupling $C^{(\mu,\nu)}_{\mathrm{R}} = 20$, detuning $\delta^{\mu} = -20$ for $N = 2$ (-40 for $N = 4$))

the environment. In rotating wave approximation the local Hamiltonian of node μ can be expressed as ($\mu = 1, 2, 3, 4$):

$$\hat{H}(\mu) = \frac{1}{2}\,\delta^{\mu}\,\hat{\lambda}_3(\mu) + \frac{1}{2}\,g^{\mu}\,\hat{\lambda}_1(\mu)\,. \tag{46}$$

The external fields are characterized by the Rabi frequencies g^{μ} and the energy difference between the laser photons and the spin energy is denoted by δ^{μ}.
The interaction between the spins will be given by the non-resonant coupling,

$$\hat{H}(\mu,\nu) = -\frac{1}{2}C_R^{(\mu,\nu)}\,\hat{\lambda}_3(\mu)\otimes\hat{\lambda}_3(\nu)\,, \tag{47}$$

which leads to an energy shift of one subsystem depending on the state of the other. In the following we will call a network "homogeneous" if all model parameters (including those for the bath coupling) are invariant under any subsystem–index permutation.

5.2 Bath model

In addition to the Hamiltonian model, we have to specify the coupling to the environment leading to decoherence effects. For simplicity we will take into account only dissipation of energy into the bath with rate $W^{\mu}_{\downarrow}$ and operator $\hat{L}_{\downarrow}(\mu) = \hat{P}_{12}(\mu)$ and for the case of a bath with finite temperature also excitations out of the bath with rate $W^{\mu}_{\uparrow}$ and operator $\hat{L}_{\uparrow}(\mu) = \hat{P}_{21}(\mu)$

In the case of a bath temperature $T = 0$ there are only jumps into the ground state, from where only the coherent laser field can drive the state out again. Therefore the distribution functions for jump- and inter-jump distances are virtually identical. For small environmental influence the broad distribution reaches its maximum at $D^2_{\psi\psi'} = 2$, due to the fact, that jumps (photon emissions) most likely start from the upper level in which case the jump into the ground level has (squared) distance 2. Increasing the ratio W/g raises the probability for jumps already for incomplete excitation, which results in a (squared) jump distance smaller than 2. In the high damping limit, the jump distance peaks at zero and the distribution becomes narrow (see Fig. 2).

The jump-distribution function $f(D^2)$ for homogeneous networks shows a scaling behavior which is only weakly dependent on size N (Fig. 2). Contrary to naive expectation, the limit $N \to \infty$ thus does not necessarily mean a classical limit. For $W/g \gg 1$ the dynamics is virtually suppressed.

The distribution changes completely, if the bath also causes excitations (bath temperature $T \neq 0$). Now, classical trajectories result, if the jump-distance distribution peaks at $D^2 = 2$ and becomes very narrow, while the inter-jump distances tend to zero (Fig. 3 and Fig. 4). This happens for $W/g \gg 1$; it will always happen for incoherent driving.

5.3 Influence of entanglement

We may truncate the expansion of correlation functions at a certain level, c, i.e. we neglect all orders of entanglement $\tilde{M}_{mlkj}$ above this specified level. This leads to a reduction of relevant state parameters (cf. Sect. 2.2), but at the same

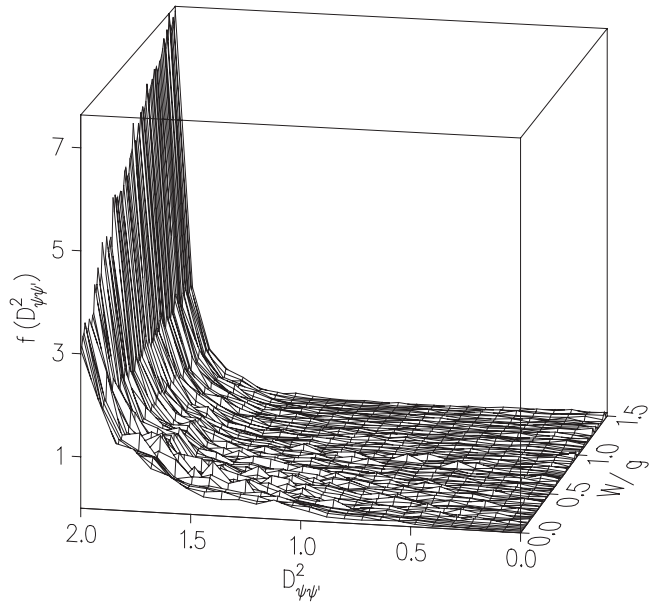

Fig. 3. Distribution function $f(D^2_{\psi\psi'})$ for the jump distance D for a network $N = 2$ in interaction with a bath of high temperature (damping rate $W^{\mu}_{\uparrow} = W^{\mu}_{\downarrow} = W$, $g^{\mu} = g =$ coupling parameter to the coherent driving field, renormalisation coupling $C_{\mathrm{R}} = 20$, detuning $\delta^{\mu} = -20$)

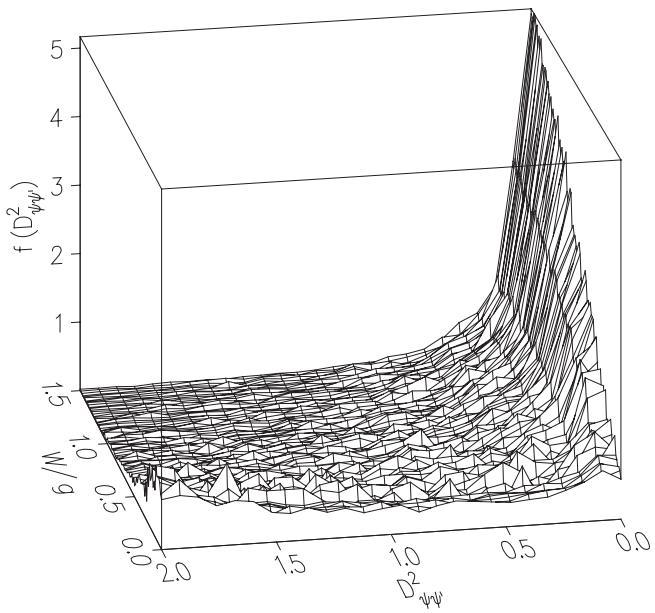

Fig. 4. Distribution function $f(D^2_{\psi\psi'})$ for the inter-jump distance, D, for a network $N = 2$ in interaction with a bath of high temperature (parameters see Fig. 3)

time to non-linear evolution equations. (For $c = 2$, we replace, for example, K_{0lkj} by the various factors as obtained from (13) with $M_{0lkj} = 0$.) As this factorization does not correspond to a concrete partitioning, those equations are not guaranteed to remain consistent. On the contrary, pure states (of closed systems) no longer remain pure, so that quantum trajectories based on this strategy lack a definite interpretation as a single-system quantum evolution. Only in the presence of sufficient damping are such deficiencies negligible.

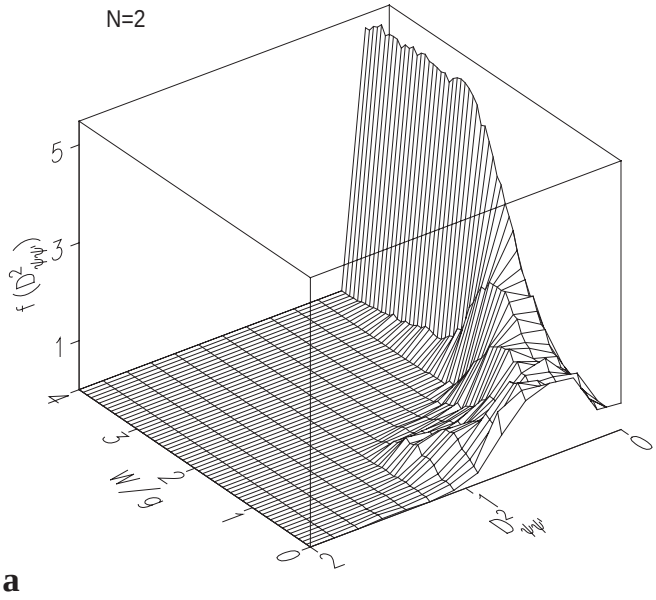

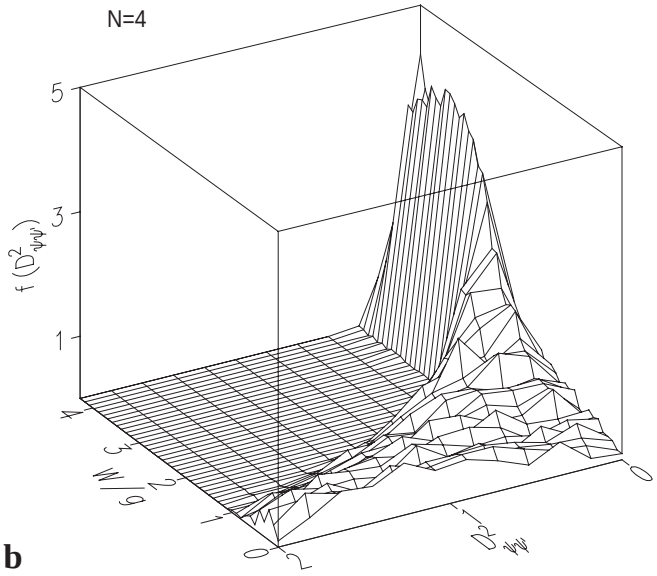

Fig. 5. Distribution function $f(D^2_{\psi\psi'})$ for the jump distance of N pseudo spins ($T = 0$), neglecting all entanglements (parameters see Fig. 2)

Alternatively, we may carry out simulations for which the state is taken to factor into concrete partitions, such as, for example, $\hat{\rho}(4, 3, 2, 1) = \hat{\rho}(4, 3) \otimes \hat{\rho}(2, 1)$. As a consequence, all entanglement terms, $\tilde{M}_{mlkj}$, between those partitioned subgroups disappear. In this case the equations of motions remain consistent, i.e. the density matrix for a closed system keeps its desired properties and a pure state stays pure. The comparison of these simulations with the exact ones then allows us to isolate the effect of various entanglements $\tilde{M}_{mlkj}$ on the level of individual quantum trajectories.

The resulting quantum trajectories are characterized as introduced for the exact ones: The respective distribution function for the jump distance is plotted in Fig. 5, where all M terms have been set to zero, a factorization into individual spins.

As we can see, increasing damping rates decrease the difference between the distributions of the exact and this factorized simulation, respectively. In the large damping regime the latter can be understood as a good approximation, which thus allows for an enormous reduction of the number of relevant state variables.

For homogeneous systems adequate factorizations should also be permutation-symmetric with respect to subsystem indices. The only candidates then are truncation schemes. In Fig. 6 we show an example for $N = 4$ where all entanglement terms beyond second order ($c = 2$) are set to zero. Nominally, this approach should constitute an improvement over the results of Fig. 5, for which all entanglement has been neglected. Qualitatively, the distribution of Fig. 6 is, indeed, between the exact and the non-entanglement result.

However, its significance is difficult to assess, as for $W/g \gg 1$ entanglement becomes negligible, anyway, while for $W/g \to 0$ the truncation scheme becomes inconsistent. In this region the jump distance may assume values greater than 2, which has no physical meaning.

On the other hand, there are examples in which the suppression of entanglement can affect quantum trajectories even in a qualitative way. This is demonstrated in Fig. 7 for an inhomogeneous $N = 2$ network. Whereas the exact evolution develops an apparently classical telegraph signal between "light" and "dark" periods ("Zenon effect", [20]), which appear to be discontinuous only on a large time scale, these transitions vanish, if entanglement is suppressed! Figure 7 shows a section of the quantum trajectories with and without entanglement and the distribution function of the state distance D^2_τ, referring to a suitable time scale ($\tau \geq 1/W$). The exact simulation has a peak for $D^2_\tau \to 0$, which is missing in the approximation.

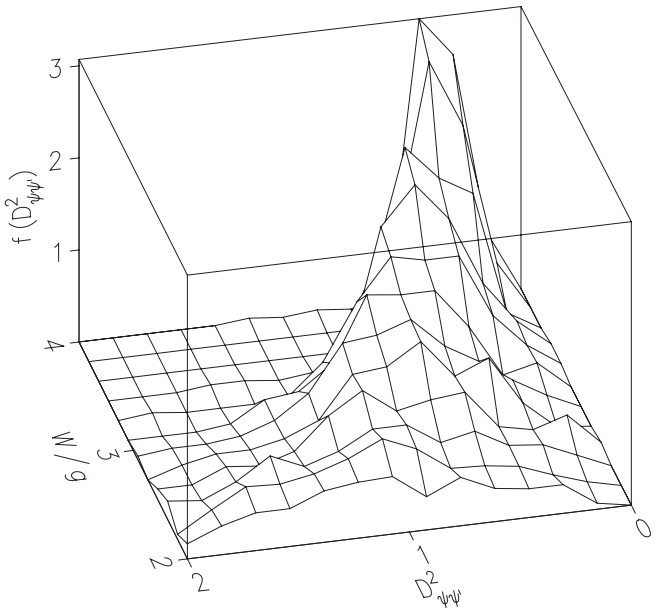

Fig. 6. Distribution function $f(D^2_{\psi\psi'})$ for the jump distance of $N = 4$ pseudo spins ($T = 0$), neglecting all entanglements beyond second order (parameters see Fig. 2)

5.4 Co-jump distribution

We finally address the non-locality in quantum trajectories. Using the concept of co-jumps we investigate the distribution function of the state changes in the respective non-projected (non-measured) part of the system. This part changes stochastically from jump to jump; we therefore denote the respective co-jump-distance as $D^{(\mathrm{red.})}$. Figure 8 shows this entirely non-local effect for $N = 2$ and $N = 4$. As one can see, entanglement is still present even in the regime of $W/g \gtrsim 4$, where the jump- and inter-jump distribution functions already indicate a rather "classical" behavior. Whereas the classicality of states implies the classicality of trajectories, the inverse is not true, in general.

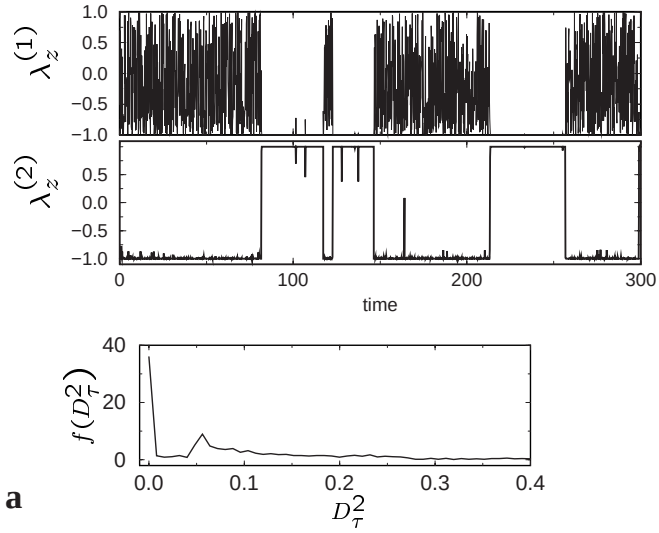

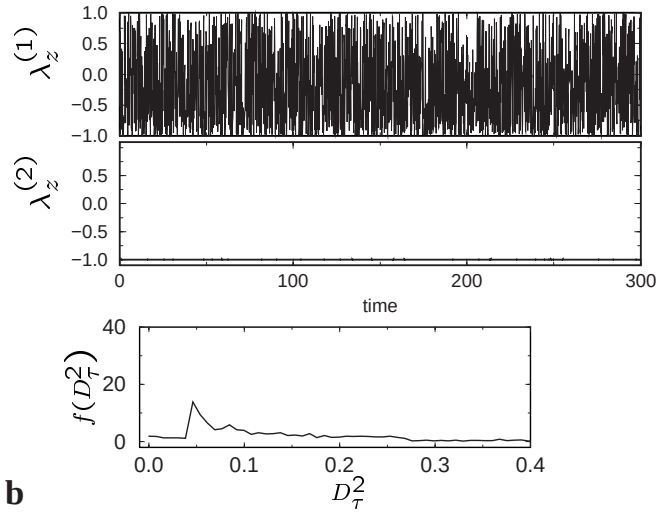

Fig. 7a,b. Trajectories of a two-spin system and its distribution function $f(D^2_\tau)$ for the exact simulation (**a**) and with neglect of entanglement (**b**); parameters: $W^1_\downarrow = 1.0$, $g^1 = 0.7$, $g^2 = 0.03$, $\delta^1 = \delta^2 = -20$, $C_\mathrm{R} = 20$, $\tau = 1.5$

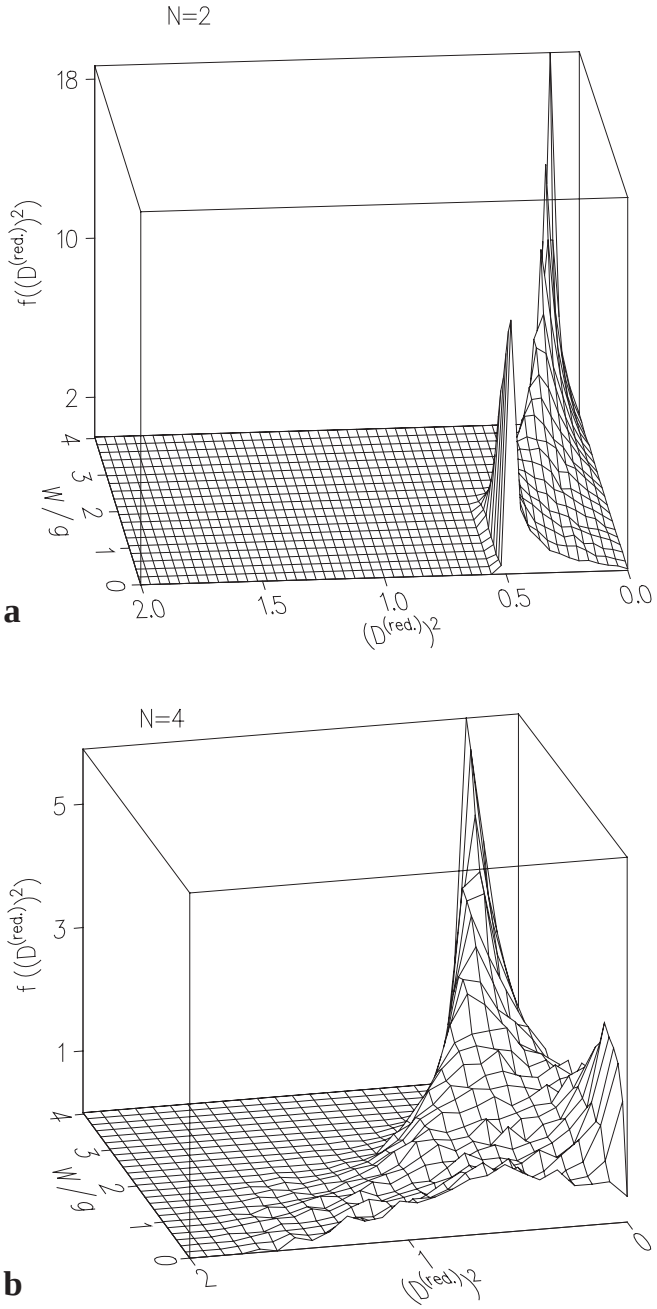

Fig. 8. Distribution function f for the co-jump distance $(D^{(\mathrm{red.})})^2$ of N pseudo spins ($T = 0$) (parameters see Fig. 3)

6 Summary and conclusions

We have investigated quantum trajectories of networks with up to $N = 4$ subsystems in terms of various statistical state-distance distributions. We have found that jump- and inter-jump distributions allow us to describe the classical limit as well as deviations from this limit in a transparent way. Other measures (such as entanglement measures) provide supplementary information.

The classification of quantum trajectories concerning non-classicality has to be distinguished from the study of non-classicality of states. Dynamic properties of open quantum systems have been investigated in terms of state changes due to quantum jumps and due to the continuous evolution. The co-jump distribution may indicate non-classicality of states despite the fairly classical trajectories.

For this analysis we found it necessary to abandon the "ignorance interpretations" of non-locality, which are often applied in quantum-information scenarios. Non-locality with respect to *individual* pure-state trajectories is, instead, introduced in an operational way, namely in terms of co-jumps.

In general, large quantum networks do not necessarily behave "classical". In the strong damping limit, "classical trajectories" ("telegraph signals") result (for a bath temperature $T > 0$) which means that the state space available to the quantum network is extremely compressed. This can be exploited for approximation schemes. However, some caution should be exercised, as truncation schemes (factorization beyond a certain level c), can lead to inconsistencies for small damping.

Acknowledgements. We thank R. Wawer, A. Otte, and I. Kim for valuable discussions. Financial support by the Deutsche Forschungsgemeinschaft is gratefully acknowledged.

References

1. H. Carmichael: *An Open Systems Approach to Quantum Optics* (Springer, Berlin, Heidelberg 1993)
2. J. Dalibard, Y. Castin, K. Mølmer: Phys. Rev. Lett. **68**, 580 (1992)
3. H. Grabert, P. Schramm, G.L. Ingold: Phys. Rev. **168**, 115 (1988)
4. H.P. Breuer, F. Petruccione: J. Phys. A: Math. Gen. **29**, 7873 (1996)
5. V. Vedral, M.B. Plenio, M.A. Rippin, P.L. Knight: Phys. Rev. Lett. **78**, 2275 (1997)
6. S. Popescu: Phys. Rev. Lett. **72**, 797 (1994)
7. A. Peres: Phys. Rev. Lett. **77**, 1413 (1996)
8. R.F. Werner: Phys. Rev. A **40**, 4277 (1989)
9. K. Vogel, V.M. Akulin, W.P. Schleich: Phys. Rev. Lett. **71**, 1816 (1993)
10. G. Mahler, V.A. Weberruß: *Quantum Networks: Dynamics of Open Nanostructures* (Springer, Berlin, Heidelberg 1998)
11. G. Mahler, R. Wawer: Superlattices Microstruct. **21**, 7 (1997)
12. M. Hübner: Phys. Lett. A **163**, 239 (1992); M. Hübner: Phys. Lett. A **179**, 226 (1993)
13. R. Josza: J. Mod. Opt. **41**, 2315 (1994)
14. M. Brune et al.: Phys. Rev. Lett. **77**, 4887 (1996)
15. M. Reed, B. Simon: *Methods of Modern Mathematical Physics*, Vol. 1: *Functional Analysis* (Academic Press, New York 1972)
16. N.G. van Kampen: *Stochastic Processes in Physics and Chemistry* (North Holland, Amsterdam 1981)
17. M.A. Nielsen, C.M. Caves: Phys. Rev. A **55**, 2547 (1997)
18. A. Aspect, P. Grangier, G. Roger: Phys. Rev. Lett. **49**, 91 (1982)
19. O. Cohen: Phys. Rev. Lett. **80**, 2493 (1998)
20. R. Wawer, M. Keller, A. Liebman, G. Mahler: Eur. Phys. J. D **1**, 15 (1998)